Favorable Monsoon Environment over Eastern Africa for Subsequent Tropical Cyclogenesis of African Easterly Waves

KELLY M. NÚÑEZ OCASIO,[a] ALAN BRAMMER,[b] JENNI L. EVANS,[c,a] GEORGE S. YOUNG,[a] AND ZACHARY L. MOON[a]

[a] *Department of Meteorology and Atmospheric Science, The Pennsylvania State University, University Park, Pennsylvania*
[b] *Cooperative Institute for Research in the Atmosphere, Colorado State University, Fort Collins, Colorado*
[c] *Institute for Computational and Data Sciences, The Pennsylvania State University, University Park, Pennsylvania*

ABSTRACT: Eastern Africa is a common region of African easterly wave (AEW) onset and AEW early life. How the large-scale environment over East Africa relates to the likelihood of an AEW subsequently undergoing tropical cyclogenesis in a climatology has not been documented. This study addresses the following hypothesis: AEWs that undergo tropical cyclogenesis (i.e., developing AEWs) initiate and propagate under a more favorable monsoon large-scale environment over eastern Africa when compared with nondeveloping AEWs. Using a 21-yr August–September (1990–2010) climatology of AEWs, differences in the large-scale environment between developers and nondevelopers are identified and are proposed to be used as key predictors of subsequent tropical cyclone (TC) formation and could inform tropical cyclogenesis prediction. TC precursors when compared with nondeveloping AEWs experience an anomalously active West African monsoon, stronger northerly flow, more intense zonal Somali jet, anomalous convergence over the Marrah Mountains (region of AEW forcing), and a more intense and elongated African easterly jet. These large-scale conditions are linked to near-trough attributes of developing AEWs that favor more moisture ingestion, vertically aligned circulation, a stronger initial 850-hPa vortex, a deeper wave pouch, and arguably more AEW and mesoscale convective systems interactions. AEWs that initiate over eastern Africa and cross the west coast of Africa are more likely to undergo tropical cyclogenesis than those initiating over central or West Africa. Developing AEWs are more likely than nondeveloping AEWs to be southern-track AEWs.

KEYWORDS: Africa; Waves, atmospheric; Monsoons; Thermodynamics; Statistical techniques; Tropical variability

1. Introduction

African easterly wave (AEW) intensification and tropical cyclogenesis (TCG) remain a challenge to explain and predict. This challenge is partly due to the limited understanding of the interactions between the mesoscale convection and synoptic environment of the AEWs. These interactions can cause variations in the structure and amplitude of AEWs as they propagate over Africa and into the Atlantic Ocean (Berry et al. 2007; Janiga and Thorncroft 2013, 2016; Cheng et al. 2019). These interactions can also cause variations when comparing AEWs that undergo TCG [i.e., developing AEWs (DAEWs)] with nondeveloping AEWs (NDAEWs).

Climatologically, DAEWs tend to have stronger low-level circulation over the west coast of Africa and the main development region (MDR) over the eastern North Atlantic, when compared with NDAEWs (Hopsch et al. 2010). Over western Africa, DAEWs are more likely to have a larger number of mesoscale convective systems (MCSs) with larger cloud area embedded within them than NDAEWs (Núñez Ocasio et al. 2020). Zawislak and Zipser (2014) showed that convective coverage is a better predictor of TCG than convective intensity. In addition, Núñez Ocasio et al. (2020) found that MCSs coupled to DAEWs are more likely to be in phase with the wave circulation than MCSs of NDAEWs, consistent with Wang (2018) who suggested that organized convection near the wave pouch center is a key feature of convection for TCG.

The wave pouch, as described by Dunkerton et al. (2009) in an attempt to explain TCG, is a circulation region within a wave-critical layer with persistent convection, vorticity, and moistening; this corresponds to consistent phasing between the convective system and wave propagation, consistent with the findings of Núñez Ocasio et al. (2020).

Another distinct feature of AEWs that undergo TCG is that the total raining area near the circulation increases during pregenesis (Zawislak 2020). Using a Lagrangian framework following DAEWs and NDAEWs, Peng et al. (2012) showed that DAEWs exhibit larger moisture content between 950 and 400 hPa than NDAEWs. On a larger scale, Brammer and Thorncroft (2015) showed that DAEWs undergo a distinct moisture ingestion in the northwest quadrant of the trough as they leave the west coast of Africa. Altogether, these studies provide evidence that DAEWs can have distinct characteristics from NDAEWs.

With regard to how AEW track pertains to TCG, Hankes et al. (2015) found that TCG is more likely with the merger of a pair of AEWs following northern and southern tracks (e.g., Reed et al. 1977; Pytharoulis and Thorncroft 1999; Thorncroft and Hodges 2001), as the merger leads to a stronger and deeper wave pouch (Dunkerton et al. 2009; Raymond and López Carrillo 2011; Wang et al. 2012). They found that this is true even for the DAEWs that subsequently undergo merging that have weaker initial circulations when compared with those of NDAEWs. Hankes et al. (2015) also found that DAEWs are associated with a stronger heat low over West Africa that extends the African easterly jet (AEJ) into the Atlantic and consequently favors further development of the DAEWs. Recently, Russell et al. (2017) proposed to use eddy kinetic energy

(EKE) at the lower levels of southern-track AEWs rather than genesis number for tropical cyclone (TC) prediction as EKE provides a measure of both AEW intensity by convectively generated circulation at the low levels and genesis number. Hence, although the AEW track has been well documented, only a few studies thus far have linked AEW track with TCG.

Elless and Torn (2019) and Torn (2010) have indicated the importance of environmental differences for AEW intensity predictability: AEW intensity forecasts with low skill are characterized by higher relative humidity values downstream of the AEW trough (Elless and Torn 2019), while short-lead-time forecasts are sensitive to the near profile of the AEW, such that higher equivalent potential temperature near the AEW results in a more intense AEW forecast (Torn 2010). Such a thermodynamic environment conducive to AEW intensification was found for the MCSs that initiated the AEW that later became Debby (2006) (Lin et al. 2013). During the initiation of pre-Debby, the monsoon trough was collocated with a cyclonic vorticity anomaly resulting from the convergence of northeasterly shamal winds and Somali jet. Vizy and Cook (2003) demonstrated that fluctuations of the large-scale environment over eastern Africa are linked to the intensity of the monsoon trough and the south-southwesterly Somali jet.

Differences between DAEWs and NDAEWs over western Africa have been well documented (e.g., Dunkerton et al. 2009; Zipser et al. 2009; Hopsch et al. 2010; Zawislak and Zipser 2010; Raymond and López Carrillo 2011; Wang et al. 2012; Zawislak and Zipser 2014; Leppert et al. 2013; Brammer and Thorncroft 2015; Russell et al. 2017; Wang 2018; Núñez Ocasio et al. 2020; Duvel 2021). Case studies, such as those of Debby in 2006 (Lin et al. 2013), Alberto in 2000 (Lin et al. 2005), Helene in 2006 (Schwendike and Jones 2010), and those focused on a more idealized numerical modeling framework (e.g., Thorncroft et al. 2008), have hinted at a possible connection between the eastern Africa large-scale conditions and TCG likelihood. Climatologically, AEW onset and AEW early life commonly occur in eastern Africa, yet the link between the large-scale environment in this region to the likelihood of an AEW subsequently undergoing TCG in a climatological sense has not been documented. In this work we will test the hypothesis that DAEWs initiate and propagate under a more favorable dynamic and thermodynamic [as it relates to the West African monsoon (WAM)] large-scale environment over eastern Africa when compared with NDAEWs. The WAM surface and low-level shear and moisture can reach eastern Africa as it will be shown in this work. This more favorable environment supports the further intensification and ultimately TCG of DAEWs. This would imply that the decrease in skillfulness noted by Elless and Torn (2019) begins at early life of the AEW and/or onset over East Africa. Based upon this substantial, but incomplete, body of knowledge, we hypothesize that differences in the African large-scale environment between DAEWs and NDAEWs could help explain TCG likelihood and may be key to improving TCG prediction, and the environment over East Africa may be more important than previously thought.

To address this hypothesis, the first part of the analysis uses geographically defined trough-relative composites (section 3). To convey the linkage between the large scale and waves, wave-centered composites are analyzed (section 4). The ultimate goal of this paper is to document the association between the monsoon environment over eastern Africa and waves that subsequently undergo TCG (i.e., DAEWs).

2. Method

a. Data and statistical significance testing

A 21-yr August–September (1990–2010) climatology of DAEWs and NDAEWs is analyzed in this work. The total number of DAEWs and NDAEWs considered is 77 and 1084, respectively. From these total numbers, the number of DAEWs and NDAEWs included for each composite region are shown in Fig. 1. We use the AEW track dataset of Cheng (2019), which is constructed using tracking methods that are similar to those in Brammer et al. (2018). The Cheng (2019) algorithm tracks the AEWs by taking mass-weighted average of the centers of curvature vorticity at 700, 600, and 500 hPa, and relative vorticity at 850 and 700 hPa, spatially smoothed over a 300-km radius. These track data were created using the European Centre for Medium-Range Weather Forecasts (ECMWF) interim reanalysis (ERA-Interim, hereinafter ERA-I; Dee et al. 2011). AEW tracks were matched with the National Hurricane Center Atlantic Hurricane Database, version 2 (HURDAT2; Landsea et al. 2014), to identify DAEWs as in Brammer and Thorncroft (2015).

The main difference between the Cheng (2019) track data used in this work and that by Brammer et al. (2018) is that Brammer et al. (2018) used an additional variable (geopotential height at 850 hPa), curvature vorticity at 600 hPa instead 850 hPa, and a spatial smoothing radius of 400 km instead of 300 km. The changes from Brammer to Cheng favor longer tracks over the continent. DAEWs are considered up to the time step right before they undergo TCG (becoming a tropical depression), and for NDAEWs until termination. In this work, we are interested in both ways a wave can fail (death over Africa and inadequacy over the Atlantic Ocean); thus, including long-lived and short-lived NDAEWs is of relevance. To exclude those that initiate in the west Atlantic, AEWs are required to be within longitudes 45°W and 60°E for their first 48 h. The AEW terminology is used because the majority of the waves that we are considering have African origin. Note, however, that we also consider in the analysis waves that originated over the Red Sea, Saudi Arabia, Yemen, and over offshore waters of the west coast of Africa (east Atlantic), because they make part of the region in the study.

ERA-I atmospheric fields are also used to create AEW-following composites. Both datasets (AEW track data and ERA-I) have a 6-hourly temporal resolution. The decision to use only a 21-yr climatology (August–September of 1990–2010), instead of ERA-I in full, pertains to the fact that (in addition to it being two full decades) in the 1990s there was a significant improvement in observations and observational coverage that consequently aided the data assimilation. Major improvements as shared by J. Knaff (NOAA/NESDIS, 2021, personal communication) that led to more realistic reanalyses are as follows:

1) In the 1990s global geostationary coverage was available.
2) Polar-orbiting satellites provided infrared and microwave sounding capabilities, high-resolution split-window infrared
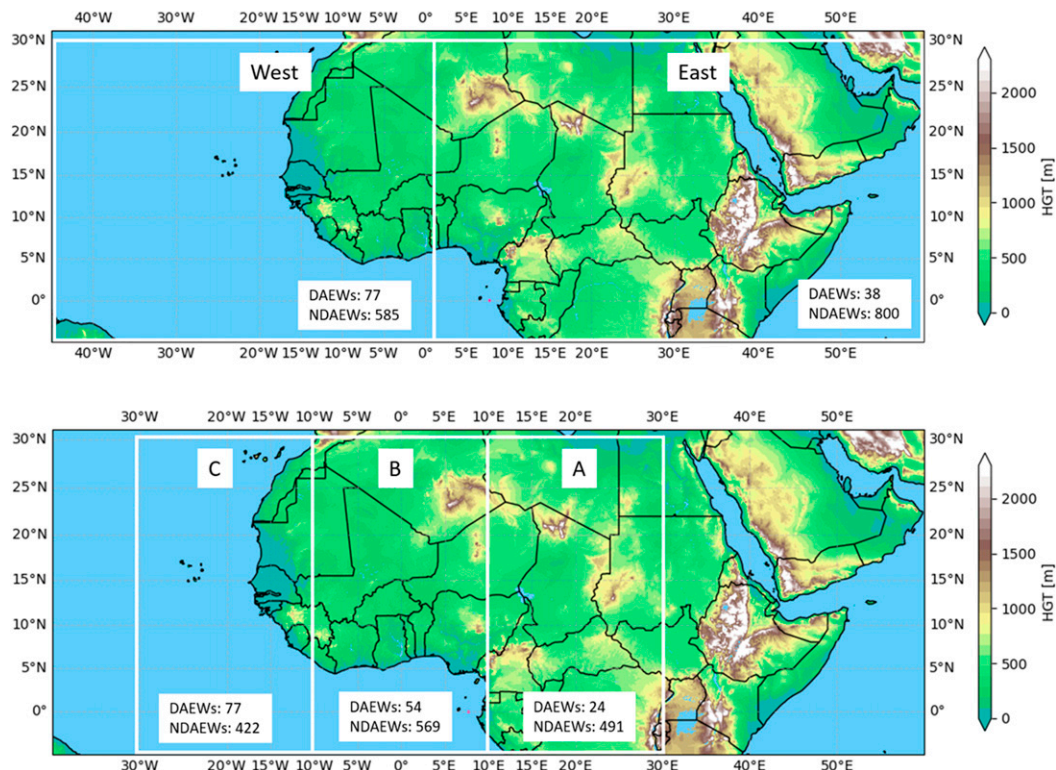
FIG. 1. (top) Domain region for geographic composites. White-outlined boxes denote regions identified as East and West. (bottom) Domain region for wave-centered composites. White-outlined boxes denote regions identified as A (east-central Africa), B (west-central Africa), and C (west coast of Africa and east Atlantic). The numbers of DAEWs and NDAEWs used for each composite region are shown in the bottom of each region.

channels, and microwave imagery, which enabled observed atmospheric temperatures, moisture, precipitation, SST, and snow cover.

3) Between late 1980 and the 1990s calibration of geostationary satellites was also significantly improved, and water vapor channels were introduced.

A bootstrapping method following Matthews and Kiladis (1999), Schreck et al. (2013), and Brammer and Thorncroft (2015) is used to test for significant differences between the DAEW and NDAEW composites. This method tests statistical significance using a two-sample t test to compare the means between 2000 randomly sampled composites of the same size. The bootstrap p values are then calculated using the Efron and Tibshirani (1993) method. The bootstrapping method takes into account the sample size of each composite as it uses the number of time steps considered for the DAEWs in each composite region to select a sample size to do the two-sample t test. To account for false significant test results, Benjamini and Hochberg (1995) false discovery rate is used with an $\alpha_{\mathrm{FDR}} = 2\alpha_{\mathrm{global}}$ (where α_{global} is the α for the t test). The dotted regions in the composites' difference plots are then significant at the 95% level. This resampling method should remove influences from any outliers in the composites and provide a reliable assessment of where the mean composites are consistently different.

b. Large-scale geographic composites

The geographic composites are done over two defined regions: *East*, which encompasses latitudes from 5°S to 30°N and longitudes from 1°W to 60°E, and *West*, which includes longitudes from 1° to 45°W (Fig. 1, top). The number of DAEWs and NDAEWs included for each composite region is also shown in Fig. 1. The way the geographic composites are built is by grouping DAEWs and NDAEWs on whether the trough center position at a particular time is over region East or region West. An example of how the grouping is done follows. If the trough of a particular DAEW (A1) is positioned over region East for three consecutive time steps, the time-average period of A1 over region East is calculated. The composite mean of variable X for DAEWs over the region East will then include a contribution from the time-average of A1's lifetime over region East. Thus, the composite mean (e.g., Figs. 2a–c for DAEWs) is the mean over all of the time-averaged DAEW periods. The same is done for NDAEWs to generate composites of the environment of DAEWs and NDAEWs that can be studied relative to their position over Africa.

c. Wave-centered composites

The wave-centered (trough centered) composites are similar to the geographic composites because they are a wave-centered mean over all the time-averaged AEW periods
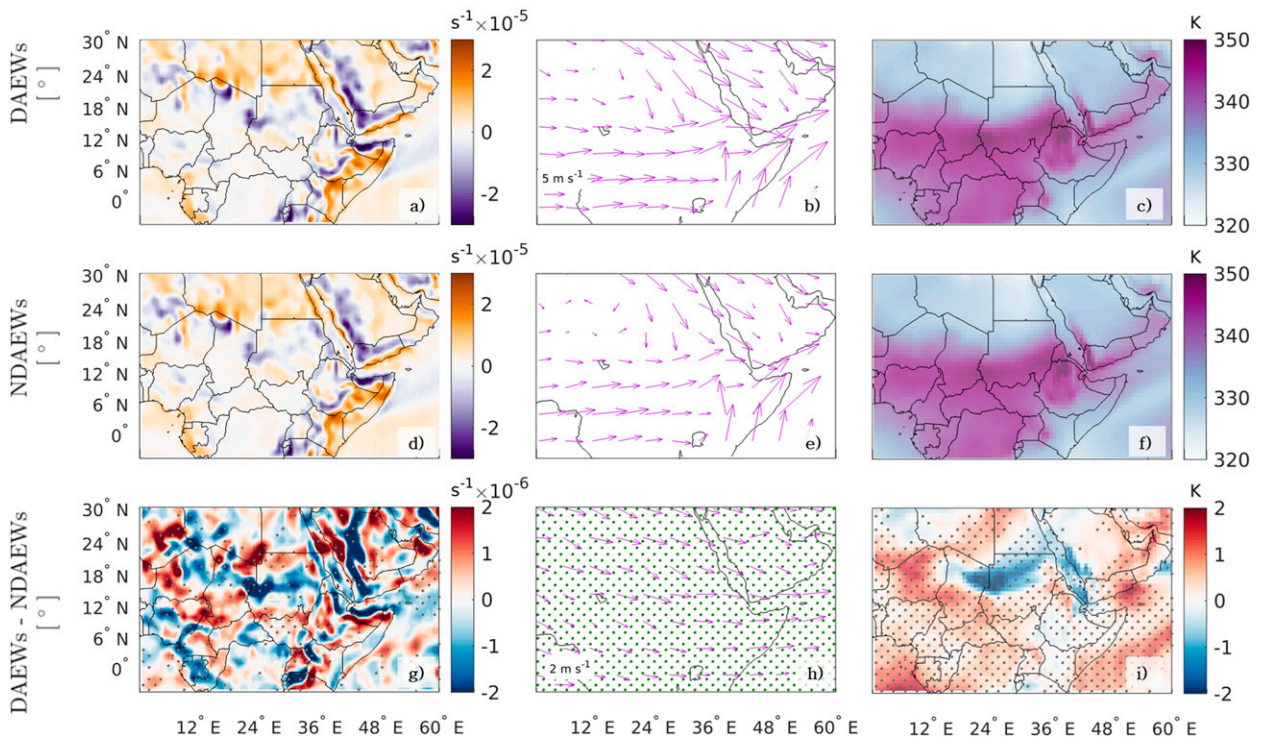
FIG. 2. Geographic composites over region East of (left) divergence, (center) 850-hPa trough-relative flow, and (right) 850-hPa θ_e for (a)–(c) DAEWs and (d)–(f) NDAEWs. (g)–(i) The difference between composites (DAEWs − NDAEWs). Stippled areas in the difference plots are significant at the 95% level.

grouped by region. However, the wave-centered regions are smaller than those of the geographic composites to be able to detect the near-trough environment. Figure 1 (bottom) shows region A (east-central Africa), B (central-west), and C (west coast of Africa and offshore waters), as well as the number of DAEWs and NDAEWs included for each composite region. Note that the wave-centered composites need not be centered on the geographic center of each region. Nonetheless, for a DAEW to be part of the region A composite, for example, the trough center would have to be located at least once within region A.

3. East and West Africa large-scale environment

Typical northern summer conditions over tropical East Africa are shown in Fig. 2 with the 850-hPa WAM flow between 5° and 15°N evident from the trough-relative flow (subtracting the AEW propagation speed from the flow) composites for DAEWs (Fig. 2b) and NDAEWs (Fig. 2e). Over region East, both DAEWs and NDAEWs experience northerly flow, cross-equatorial flow from the southern Indian Ocean and the Somali jet all converging over Ethiopia and Somalia consistent with the Vizy and Cook (2003) climatology. The low-level moisture signature of the monsoon is evident from the 850-hPa equivalent potential temperature θ_e composites of both DAEWs (Fig. 2c) and NDAEWs (Fig. 2f). The 850-hPa divergence composites of both DAEWs and NDAEWs are shown in Figs. 2a and 2d, respectively.

The difference between the 850-hPa trough-relative flow composites (Fig. 2h) reveals stronger northerly flow and WAM

flow, and a stronger zonal Somali jet for DAEWs. Dotted areas in Figs. 2g, 2h, and 2i are areas where DAEWs and NDAEWs are significantly different at 95% confidence. The stronger westerly monsoon flow for DAEWs (2–4 m s^{-1} stronger) penetrates more into the Somali jet over eastern Africa. The combination of stronger northerly and westerly monsoon flow for DAEWs is associated with a region of significantly stronger convergence for DAEWs over the Marrah Mountains and is shown in Fig. 2g (around 24°E and 15°N). The difference over this region is of importance giving that Thorncroft et al. (2008) showed that the heating by convective triggers in the vicinity of the Marrah Mountains (previously known as Darfur Mountains), the entrance region of the AEJ, can force AEW. Other studies have shown the importance of topography for AEW forcing and energetics (e.g., Lin et al. 2005; Schwendike and Jones 2010; Hamilton et al. 2020).

The difference between the 850-hPa θ_e composites (Fig. 2i) show that AEWs have significantly larger WAM low-level moisture and/or warmer conditions especially downstream of the Marrah Mountains (south of Chad and Niger; red stippled shading in Fig. 2i). However, just north of the Marrah Mountains, DAEWs actually experience cooler and/or drier conditions than the NDAEWs (from −1.5 to −2 K lower than NDAEWs; blue shading in Fig. 2i). These lower values of θ_e for DAEWs just north of the Marrah Mountains are associated with a suppression of deep convection, as shown in Fig. 3f, and a decrease in 850-hPa relative humidity (not shown). We hypothesize that 1) the WAM experienced by DAEWs is
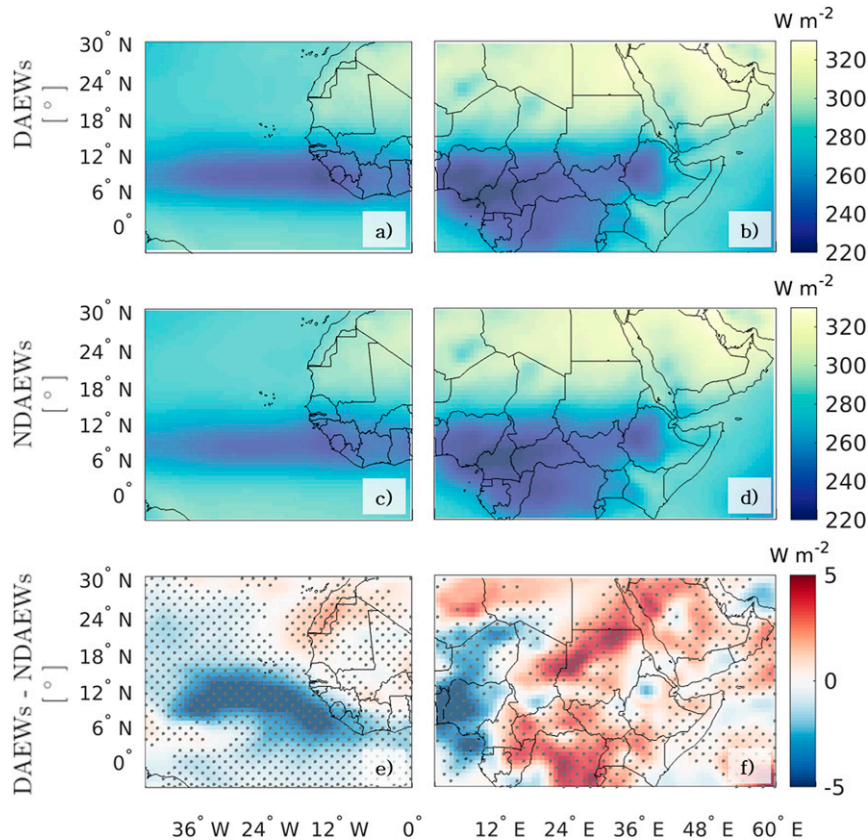
FIG. 3. Geographic composites for (right) region East and (left) region West of OLR (color shades) for (a),(b) DAEWs and (c),(d) NDAEWs. (e),(f) The difference between composites (DAEWs − NDAEWs). Stippled areas in the difference plots are significant at the 95% level.

concentrated closer to the equatorial belt, thus explaining the reduction of moisture north of the Marrah Mountains, and/or 2) that thermodynamic factors over eastern Africa and especially the region around the Marrah Mountains may not be playing a major role in the initiation and early life of DAEWs over eastern Africa. We note that the more active WAM for DAEWs favors enhanced convection (Fig. 3f) west of 12°W, concentrating downstream the of the Cameroon Highlands over Nigeria. This suggests that interactions of DAEWs with MCSs are more favored over central Africa.

Leroux and Hall (2009) showed that other dynamical factors such as vertical shear and the strength of the AEJ can be important for forcing AEWs, not just the convective triggers over the Marrah region. The analysis presented here agrees with Leroux and Hall (2009) in that localized low-level anomalous convergence, a dynamical factor, could be a major contributing factor for AEW forcing, especially for those AEWs that undergo TCG with triggering of the organized convective systems farther downstream of the Marrah Mountains. Furthermore, we show that these optimal localized low-level anomalous convergence conditions experienced by DAEWs as they are forced or initiated over the Marrah Mountains are more likely when westerly monsoon flow is stronger than the westerly monsoon flow experienced by NDAEWs (Fig. 2h).

The AEJ is evident in composites of 950–650-hPa zonal bulk shear over region West for both DAEWs (Fig. 4a) and NDAEWs (Fig. 4d). The difference between the composites reveals a more intense and elongated AEJ for DAEWs, reflected by stronger easterly shear for DAEWs off the West African coast and by its extension into the tropical east Atlantic (Fig. 4g). This more intense and extended AEJ for DAEWs was also seen in Hankes et al. (2015) study for DAEWs. DAEWs experience a statistically significant stronger WAM flow over region West than NDAEWs (Fig. 4h). Off the west coast of Africa and farther into the MDR, the difference in the 850-hPa θ_e composites depicts a larger area of higher values for DAEWs (Fig. 4i) than for NDAEWs. These higher values are associated with the extension of the AEJ and partly, to the deep convection associated with the DAEWs (Fig. 3e).

Recall that DAEWs are AEWs that result in the formation of a tropical depression off the west coast of Africa, so all DAEWs will leave the west coast of Africa ("leave WC"), no matter in which region they form (Table 1, column 2). Only some NDAEWs cross the coast, but since NDAEWs are far more numerous they still represent the vast majority of coastal systems (Table 1, columns 3 and 4). The probability of DAEWs leaving the coast for each composite region is computed as
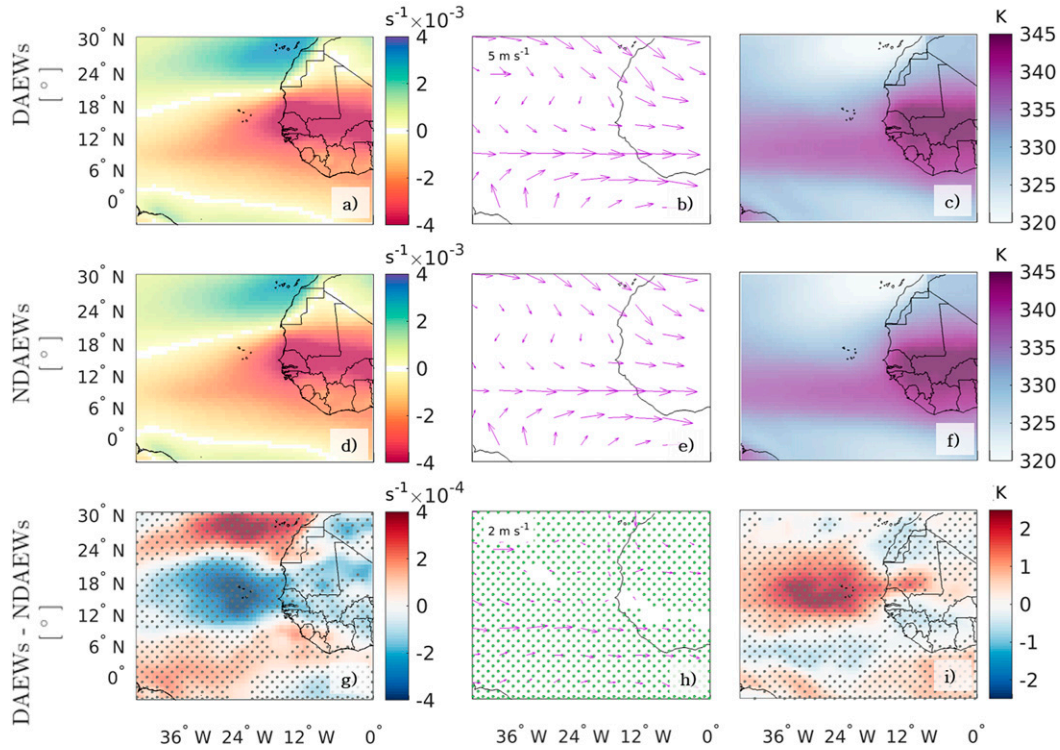
FIG. 4. Geographic composites over region West of (left) 950–650-hPa zonal bulk shear, (center) 850-hPa trough-relative flow, and (right) θ_e for (a)–(c) DAEWs and (d)–(f) NDAEWs. The zonal bulk shear is the horizontal shear of the bulk layer zonal wind and is calculated by taking the difference of the magnitude of the zonal wind at 950 and 650 hPa over the geopotential height of the column. (g)–(i) The difference between composites (DAEWs − NDAEWs). Stippled areas in the difference plots are significant at the 95% level.

$$P(\text{DAEW}|\text{leave WC}) = \frac{P(\text{DAEW})P(\text{leave WC}|\text{DAEW})}{P(\text{leave WC})}. \tag{1}$$

Almost 90% of NDAEWs that initiate over region West cross the coast, in contrast to only 24% of NDAEWs initiating in region East (Table 1, column 3). Between AEWs that initiate over regions East and West, AEWs that initiate over region East have the highest probability of developing—over 16%—provided they cross the west coast of Africa (Table 1, row East versus row West).

When analyzing the initial position of DAEWs and NDAEWs over regions East and West we found that DAEWs initiating over region East on average initiate at 9.39°N latitude whereas region East NDAEWs initiate farther north, at 11.3°N. As mentioned above, AEWs in this climatology that initiate over region East and cross the west coast are more likely to develop than those initiating over region West. Thus, the southward shift in mean initiation latitude suggests that DAEWs are for the most part southern-track AEWs and are more likely to form over East Africa.

In summary, it is shown that there are more favorable large-scale conditions over regions East and West for DAEWs than for NDAEWs and that these conditions are linked to TCG likelihood. Over eastern Africa, DAEWs experience

1) stronger northerly and WAM flow,
2) more intense zonal Somali jet and stronger convergence over the Marrah Mountains (region of AEW forcing), and
3) larger WAM moisture and convective signature concentrated west of the Marrah Mountains.

Over western Africa, DAEWs experience

1) stronger WAM flow and
2) more intense and extended AEJ off the west coast of Africa and offshore waters.

It is also shown from statistics in Table 1 that these favorable conditions are in fact related to the waves' potential to undergo TCG downstream of the favorable environment.

TABLE 1. Fraction of DAEWs and NDAEWs that leave the west coast of Africa with respect to initiation location. The probability of DAEWs leaving the coast is also shown. Regions are defined in Figs. 1 and 2.

Region	DAEWs	NDAEWs	Pr(DAEW|leave WC)
A	21/21 = 100%	76/302 = 25.2%	21.6%
B	28/28 = 100%	212/295 = 71.9%	11.7%
C	21/21 = 100%	116/116 = 100%	15.3%
East	40/40 = 100%	197/820 = 24.0%	16.9%
West	37/37 = 100%	234/264 = 88.6%	13.7%
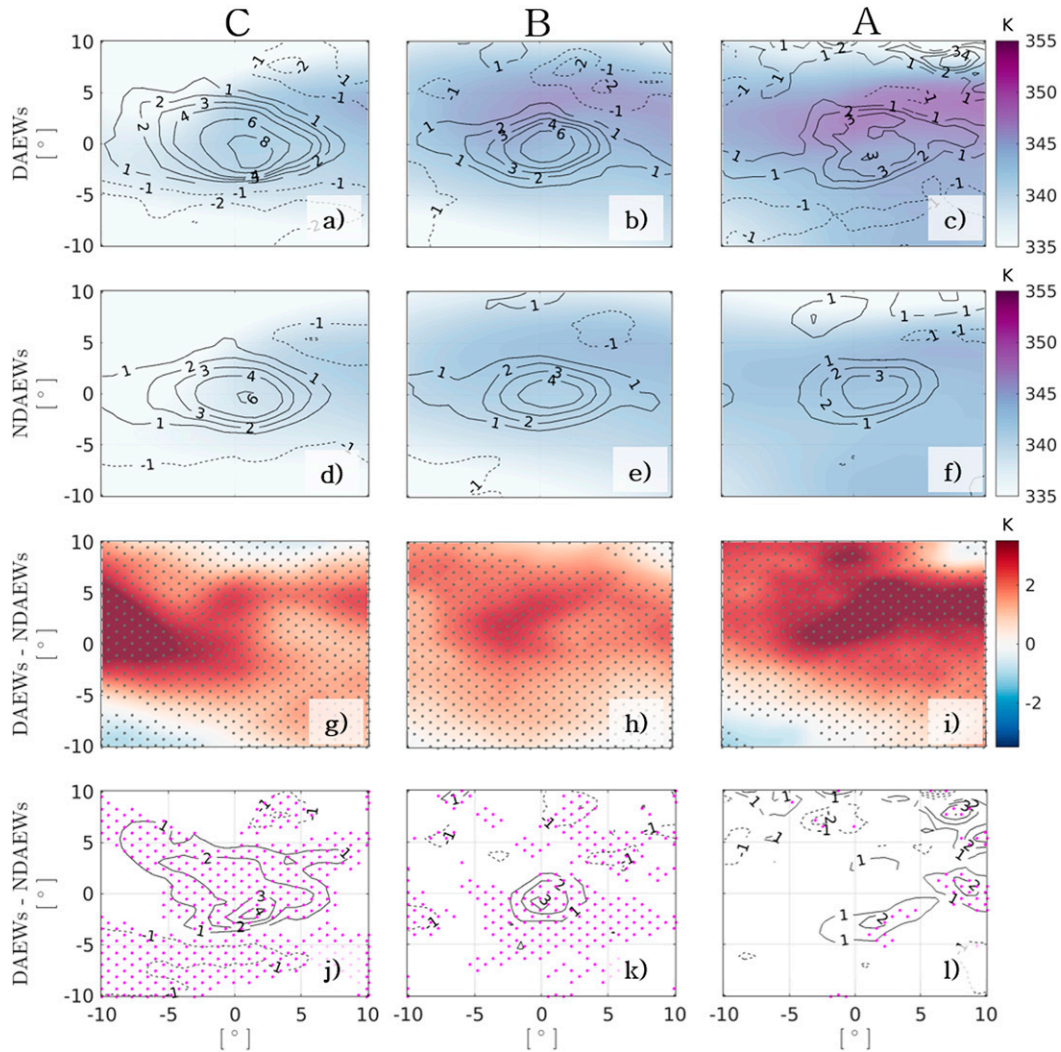
FIG. 5. Wave-centered composites for regions (right) A, (center) B, and (left) C of 850-hPa θ_e (color shades) for (a)–(c) DAEWs and (d)–(f) NDAEWs. Labeled solid black contours are 850-hPa relative vorticity ($\times 10^{-6}\,\mathrm{s}^{-1}$). (g)–(i)The difference between θ_e composites (DAEWs − NDAEWs), and (j)–(l) the difference for relative vorticity. Stippled areas in the difference plots are significant at the 95% level.

Thus, this makes possible to target an AEW as a DAEW as early as its initiating stages over eastern Africa. A case study by Lin et al. (2013) suggested that the precursor of pre-Debby (2006), were attributable to the synoptic interaction between the Shamal wind and the penetration of the Somali jet over eastern Africa. The results presented here support the Lin et al. (2013) case study, but our use of a 21-yr database of events provides more quantitative evidence of this favorable large-scale environment in addition to other conditions identified and mentioned above.

Elless and Torn (2019) and Torn (2010) have shown that the large-scale environment influences AEW intensity predictability. The analysis of the large-scale environment of DAEWs and NDAEWs here demonstrates distinct and significant differences characterized by the same environmental variables as they considered in their work. The results presented here

evidence the importance of using both western and eastern Africa large-scale environment to inform TCG prediction. To study how this favorable large-scale environment plays a role in the near-trough DAEW environment and how it compares to the NDAEW near-trough environment, wave-centered composites are examined next.

4. Near-trough environment

a. East-central Africa: Region A

Wave-centered composites of 850-hPa θ_e (shading) and relative vorticity (contours) for regions A (east-central Africa), B (central-west), and C (West Africa and offshore waters) are shown in Figs. 5a–5c for DAEWs and Figs. 5d–5f for NDAEWs. In region A, statistically significantly higher values
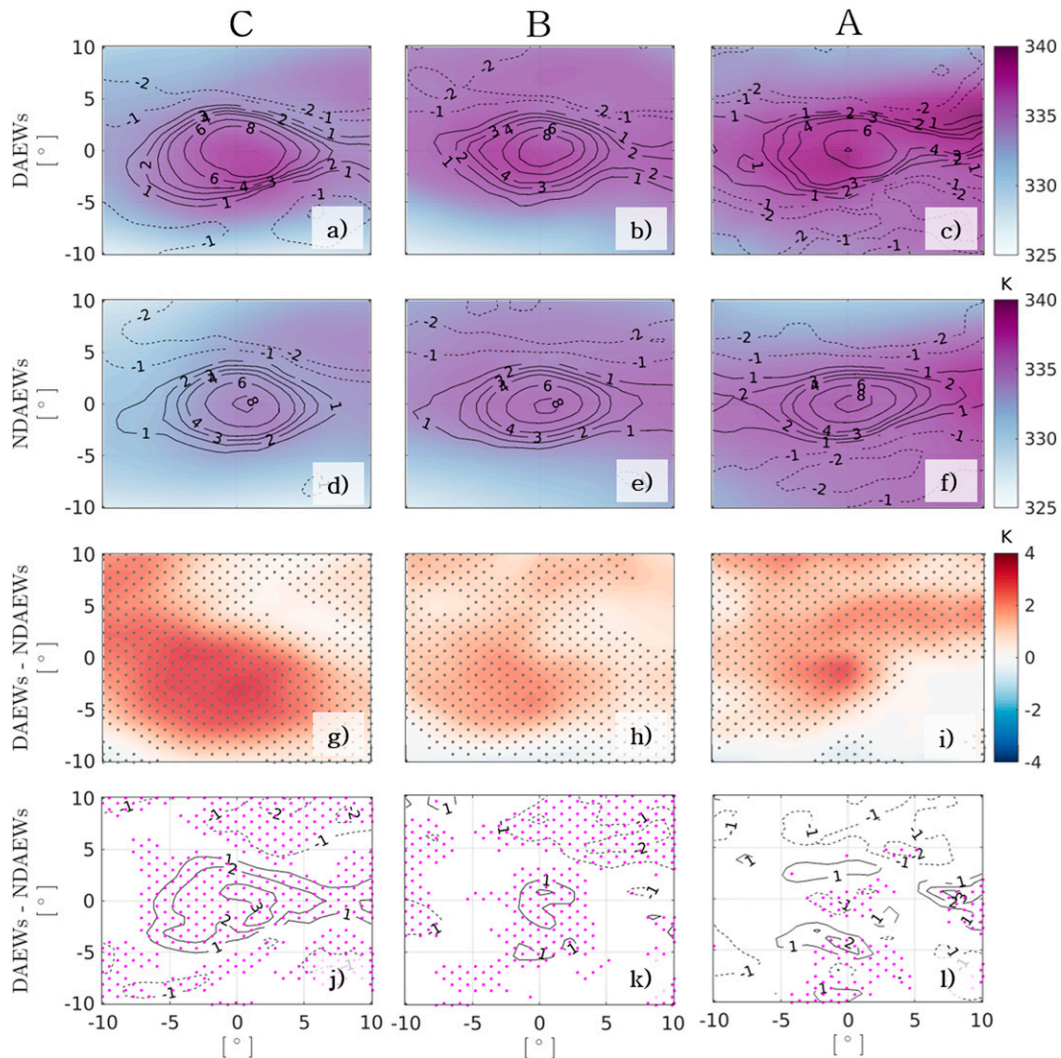
FIG. 6. As in Fig. 5, but at 700 hPa.

of 850-hPa θ_e (2 K and higher) in the northeast quadrant and center are found for DAEWs relative to NDAEWs (Fig. 5i, composite difference). This is also evident at 700 hPa (Fig. 6i, composite difference), especially in the trough center. The anomalous wave-scale flow of DAEWs is advecting the anomalously higher moisture from the monsoon environment found over region East (Fig. 2i) toward the center of the circulation. The difference in relative vorticity reveals that the average 850-hPa trough center for DAEWs in region A is slightly more intense than that of NDAEWs (Fig. 5l).

DAEWs over region A experience stronger 850-hPa convergence at the trough center than NDAEWs (Fig. 7, composite difference in Fig. 7i); these more favorable near-trough conditions are associated with the greater low-level convergence over the Marrah Mountains, a region of AEW forcing and initiation (Fig. 2h). The stronger convergence over Marrah Mountains is linked to the stronger westerly flow signature from the WAM experienced by DAEWs when compared with NDAEWs. Both DAEWs and NDAEWs at 700 hPa

experience convergence at the trough center as well (Figs. 8c,d, respectively). That DAEWs exhibit stronger 700-hPa convergence at the trough center than NDAEWs appears to affect the likelihood of DAEWs having an enclosed circulation at 700 hPa (Fig. 9c, red streamlines). Note how DAEWs have an open 700-hPa inverted trough structure (Fig. 9c, red streamlines) whereas NDAEWs have a closed circulation at both levels and more pronounced initial stacking of the 850- (blue streamlines) and 700-hPa (red streamlines) vortices. Hankes et al. (2015) found that DAEWs that subsequently undergo vortex merging and TCG have an initial shallower wave pouch (Dunkerton et al. 2009) when compared with NDAEWs, which agrees with these results as DAEWs studied here do not have a defined closed circulation at 700 hPa (Fig. 9c, red streamlines). Hankes et al. (2015), however, only considered Cape Verde storms whereas in this study waves initiating anywhere inside regions West and East are considered (domain in Fig. 1). This analysis reveals that while shallower, the stronger 850-hPa moisture-enhanced initial circulation of DAEWs are linked to
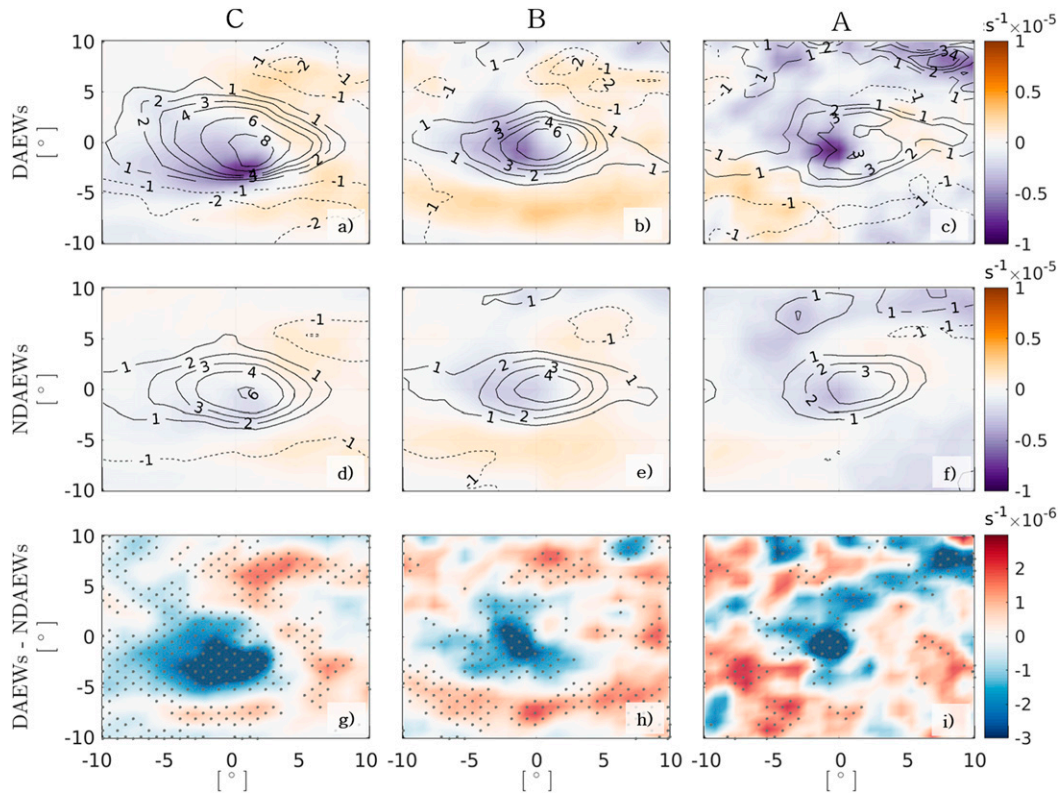
FIG. 7. Wave-centered composites for regions (right) A, (center) B, and (left) C of 850-hPa divergence (color shades) (a)–(c) DAEWs and (d)–(f) NDAEWs. Labeled solid black contours are 850-hPa relative vorticity ($\times 10^{-6}\,s^{-1}$), repeated from Fig. 5. (g)–(i) The difference between the 850-hPa divergence composites (DAEWs − NDAEWs). Stippled areas in the difference plots are significant at the 95% level.

the large-scale conditions over region East identified for DAEWs during their initiation and early life (previous section), and hence, DAEWs can have a "memory" as suspected by Núñez Ocasio et al. (2020). In support of this argument, Brammer and Thorncroft (2017) found that about 25% of the trough region recirculates within itself for five days before reaching the coast. Thus, enhanced moisture over region East is intrinsically related to the enhanced moisture near the trough of DAEWs (Fig. 7i). Another interesting feature of DAEWs over region A is that they show (statistically significant) higher values of CAPE in the northeast quadrant (Fig. 10i). However, this available energy is likely to be lost because it is over the southerlies, which is a region of adiabatic descent (Janiga and Thorncroft 2016).

The mean latitude of the wave-center composites of DAEWs (Fig. 9c, top right) and NDAEWs (Fig. 9f, top right) over region A reveal that, on average, the track of DAEWs over region A is farther south (9.3°N) than that of NDAEWs (11.2°N). Furthermore, on average, the latitude of initiation for DAEWs in A is 8.7°N, whereas for NDAEWs it is 11.8°N. Combining these statistics with the analyses in the previous section leads us to conclude that DAEWs are more likely to be southern-track AEWs. Consistent with this finding, Thorncroft and Hodges (2001) demonstrate that southern-track AEWs are known to foster moist convective systems that can support TCG.

Russell et al. (2017) suggest that the southern AEW track could be used for seasonal TC prediction. Russell et al.'s (2017) study, however, only considers AEWs as far as 10°W. In this study we find that DAEWs form 21.6% of all AEWs that initiate in A and cross the coast. Thus, the probability of a region A AEW undergoing TCG is more likely than for an AEW initiated in region B (11.7%) or C (15.3%) (Table 1, rows A, B, and C). This is the case for DAEWs initiating over region East, which includes region A, where conditions are more favorable for TCG. Thus, these results reveal the importance of considering eastern Africa large-scale conditions when predicting whether or not an AEW will undergo TCG. Moreover, the large-scale conditions identified for the early life of DAEWs in the previous section can be key predictors of TCG. Region B is shown next, to analyze how the large-scale environment becomes more important as the waves propagate over central and West Africa.

b. Central-west Africa: Region B

Higher 850- and 700-hPa θ_e values for DAEWs are evident throughout most of region B (Figs. 5h and 6h, respectively), especially in, and to the north of, the trough axis. In this region, the relative vorticity signature for DAEWs is significantly more intense than that of NDAEWs at both 850 and 700 hPa (Figs. 5k and 6k, respectively). The northerlies of AEWs are a
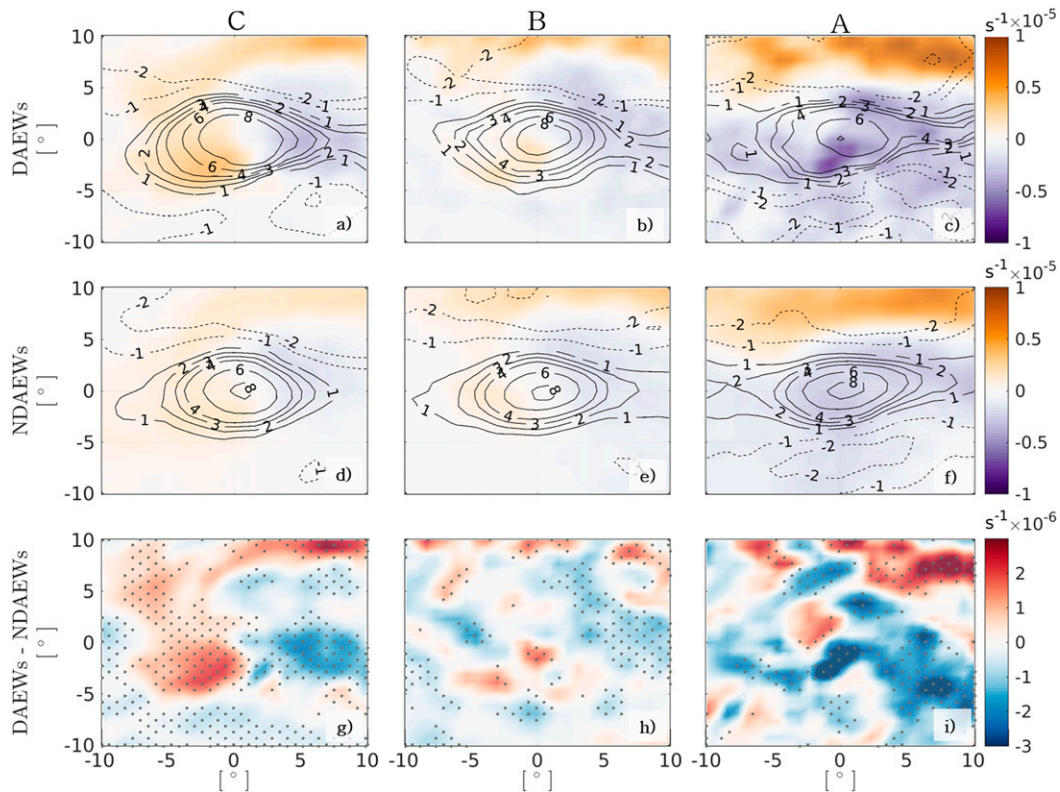
FIG. 8. As in Fig. 7, but at 700 hPa.

region of adiabatic ascent, and Janiga and Thorncroft (2016) have shown that they are also a region of positive moisture anomalies over central-west Africa (similar geographically as region B here). These results show then that the moisture anomaly is even greater for DAEWs. The region of higher moisture for DAEWs at 850 hPa (Fig. 5h) is collocated with a region of higher CAPE (Fig. 10h), which can be conducive for convective initiation. This is true for DAEWs as they have more deep convection associated with them as seen from the outgoing longwave radiation (OLR) in Fig. 3, west of 12°E. The convergence maximum associated with DAEWs in region B is aligned with the relative vorticity maximum; it is also stronger than the convergence maximum for NDAEWs (Fig. 7h). The divergence and convergence patterns are reversed at the 700-hPa level (Fig. 8) for both DAEWs and NDAEWs as expected (Reed et al. 1977). The more intense 850-hPa dynamical signature, anomalously high 850-hPa moisture and CAPE for DAEWs in region B (and A), suggest that the region just above the boundary layer plays a key role in the likelihood of TCG from an AEW. This concurs with Russell et al. (2017), who suggested that prediction of 1000–800-hPa eddy kinetic energy could be useful for prediction of TC formation.

Over region B, the amplitude of the 700-hPa DAEW inverted trough is larger (Fig. 9b, red streamlines) than that of the NDAEW trough (Fig. 9e, red streamlines). Although both DAEWs and NDAEWs exhibit a broadening of the 850-hPa circulation from region A to B (Fig. 9b, blue streamlines, and Fig. 9e, blue streamlines, respectively), the DAEWs

experience an intensification of the 700-hPa wave structure whereas NDAEWs exhibit a weakening (red streamlines). Thus, the importance of maintaining a strong 850-hPa vortex, and a vertical alignment of vortex centers for TCG as suggested by Jones (1995), Wang et al. (2012), and Raymond and López Carrillo (2011) becomes relevant over central Africa, where the eastern Africa large-scale conditions have modulated the AEW to develop a more suitable wave that undergoes TCG.

To show how the large-scale conditions identified reflect on how the AEW intensity evolves in time and transitions from region to region, Fig. 11 includes the tracks of a representative DAEW (circles) and NDAEW (triangles) and time series of the mean relative vorticity at 700 (Fig. 11b) and 850 (Fig. 11c) hPa. The position and relative vorticity value over region A, B, and C, are colored in magenta, red, and blue, respectively. Over region A (magenta), the NDAEW exhibit a stronger vortex at both 850 and 700 hPa, but as they transition from region A to region B the relative vorticity signature of the DAEW begins to surpass that of the NDAEW. For the majority of the time in region B, peak values of relative vorticity for the DAEW are between 10×10^{-8} and $16 \times 10^{-8}\,\mathrm{s}^{-1}$, while peak values at both levels remain at around 5 and $10 \times 10^{-8}\,\mathrm{s}^{-1}$ for the NDAEW. Recall that over B, DAEWs are associated with more MCSs than NDAEWs (Fig. 3f, west of 12°E) (Núñez Ocasio et al. 2020). Consistent with the large-scale conditions of the evolving DAEWs (identified above), DAEWs moving into central (and, eventually, western) Africa are increasingly interacting with MCSs. We hypothesize that this AEW–MCS
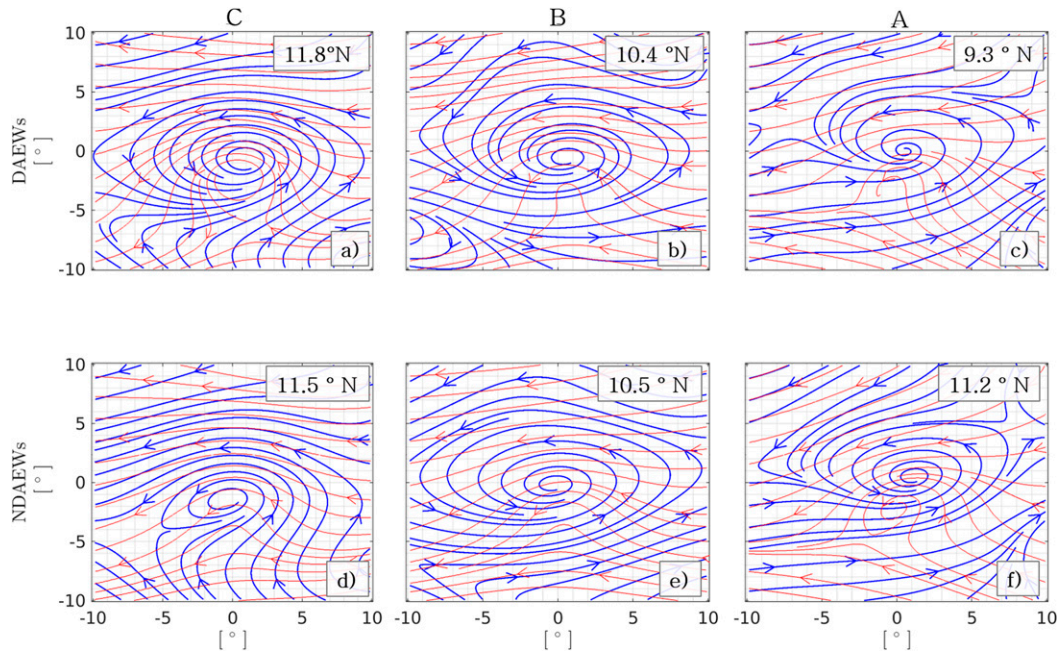
FIG. 9. Wave-centered composites for regions (right) A, (center) B, and (left) C total wind (m s^{-1}) at 850 (blue streamlines) and 700 (red streamlines) hPa for (a)–(c) DAEWs and (d)–(f) NDAEWs. The mean latitude for each composite is shown in the top-right corner.

interaction maintains and enables further intensification of the increasingly intense structure of DAEWs through diabatic potential vorticity (PV) localization. The intensity gain by the DAEW as it transitions from A to B is significant and appears to be key in maintaining, for the most part, values exceeding 10×10^{-8} s^{-1} over region C for the lower tropospheric relative vorticity anomaly that will ultimately contribute to TCG. We suggest that although both the DAEW and NDAEW were modulated by the topographic influence of the Cameroon Highlands, there is a causality between strengthening of this DAEW case over region B and the favorable large-scale conditions identified for DAEWs presented in this work.

c. West Africa and offshore waters: Region C

Analyses of the near-trough structure of DAEWs and NDAEWs over West Africa and offshore waters complete the picture of the AEW evolution described here. Over region C, DAEWs have significantly higher 850- and 700-hPa θ_e values relative to NDAEWs, especially at the trough center (Figs. 5h and 6h, respectively) and over the northerlies at 850 hPa (Fig. 5h). Over this region DAEWs experience a more intense and extended AEJ and stronger westerly monsoon flow (Figs. 4g,h). The anomalous wave-scale flow of DAEWs is likely advecting the anomalously higher monsoon moisture toward the center of the circulation. At this point the vorticity signature of DAEWs is significantly greater at both levels (Figs. 5j and 6j). Both the 850-hPa relative vorticity signature (Fig. 5a) and 850-hPa circulation of DAEWs (Fig. 9a, blue streamlines) are distinctly more elongated than those of

NDAEWs at 850 hPa. The DAEWs are now maintained by strong convergence at the 850-hPa circulation center (Fig. 7g). Additionally, DAEWs exhibit stronger convergence at 850 hPa and stronger divergence at 700 hPa than do NDAEWs (Fig. 8g) and, thus, a more intense vertically aligned vortex.

DAEWs now have a well-defined vertically aligned 850–700-hPa vortex (Fig. 9a). This vertically aligned DAEW vortex, or deep wave pouch (Dunkerton et al. 2009), can distinguish a DAEW from a NDAEW over region C and is consistent with Wang (2018) and Raymond and López Carrillo (2011) findings, yet we add to the analysis that this alignment begins over region B (central-west Africa) as it was shown in the previous section. The NDAEWs do not regain a closed circulation at 700 hPa (Fig. 9d), leaving the system open to advection of dry air into the trough center (Brammer et al. 2018). Dry air intrusion would suppress convection and therefore AEW-convection interaction and ultimately reduce the potential for TCG. Even if the initial NDAEW circulation is deeper (as shown in Fig. 9f) than of the DAEWs, favorable large-scale conditions over eastern Africa (Fig. 2) experienced by DAEWs is what ultimately preconditions them for subsequent TCG.

This optimal vertical alignment/deeper wave pouch for DAEWs, which begins to take form over region B (central-west Africa), makes DAEWs more susceptible to experience moisture vortex instability (MVI) (Adames and Ming 2018; Adames 2021). In MVI, the anomalous wave-scale flow advects moisture and temperature toward the synoptic-scale vortex. The advection creates a favorable thermodynamic environment for convection to develop near the vortex, which
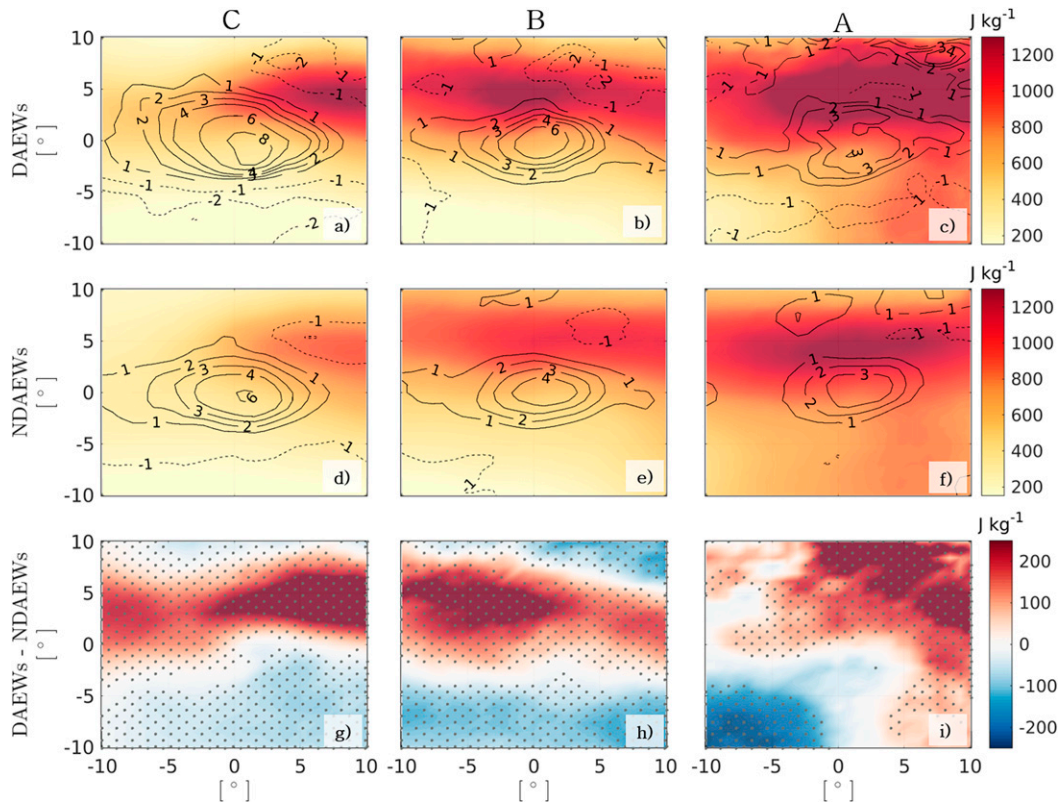
FIG. 10. Wave-centered composites for regions (right) A, (center) B, and (left) C of CAPE (color shades) for (a)–(c) DAEWs and (d)–(f) NDAEWs. Labeled solid black contours are 850-hPa relative vorticity ($\times 10^{-6}\,\mathrm{s}^{-1}$), repeated from Fig. 5. (g)–(i) The difference between composites (DAEWs − NDAEWs). Stippled areas in the difference plots are significant at the 95% level.

intensifies the vortex through vortex stretching (and thus, PV localization). The interactions between the convection and the vortex create a feedback loop that favors the growth of the coupled system. Núñez Ocasio et al. (2020) argued that MVI is much more likely for DAEWs than NDAEWs due to the phasing between convection and the wave trough for DAEW–MCS systems. They show that, not only are the MCSs of DAEWs more likely to move at the same speed of the wave trough, they are latitudinally phase locked with the wave trough. That is, MCSs are more likely located in the same latitude (or close) to the corresponding DAEW trough. In contrast, MCSs of NDAEWs tend to be located south of the NDAEW trough center. Núñez Ocasio et al. (2020) speculate that the reason for this is that, unlike NDAEWs, DAEWs remain in a moisture and AEJ enhanced environment in which the MCSs thrive and thus, AEW–MCS interactions are more likely to result in AEW intensification. The results presented here verify this hypothesis, as the stronger westerly monsoon flow and a shear-enhanced AEJ in which DAEWs propagate, both play a role in developing the convectively favorable near-trough environment.

We argue that the conditions over eastern Africa are critical for initiating an AEW that will subsequently undergo TCG. The mean latitudinal position of DAEWs and NDAEWs over central (Figs. 9b and 9e, respectively) and western Africa

(Figs. 9a and 9d, respectively) are not nearly as important for TCG as their latitude of initiation over region East (Fig. 9c). These results reveal that DAEW are more likely to be southern-track waves that initiate over eastern Africa.

5. Summary and conclusions

The objective of this study was to refine our understanding of the interconnection between the large-scale and near-trough environments in the evolution of AEWs that ultimately lead to TCG—these are the DAEWs of this study. We test the hypothesis that DAEWs initiate and propagate under a more favorable dynamic and thermodynamic (WAM) large-scale environment over eastern Africa, and that this environment is demonstrably different from the initiation environment for NDAEWs. Using a 21-yr August–September (1990–2010) climatology of AEWs, the large-scale environment of DAEWs and NDAEWs were characterized and shown to be statistically significantly different. The following are the large-scale environmental differences identified that we propose are linked to subsequent TCG events. We enumerate the differences for region East and West Africa as examined here. Over eastern Africa, DAEWs experience

1) stronger northerly and WAM flow,
2) more intense zonal Somali jet and stronger convergence over the Marrah Mountains (region of AEW forcing), and
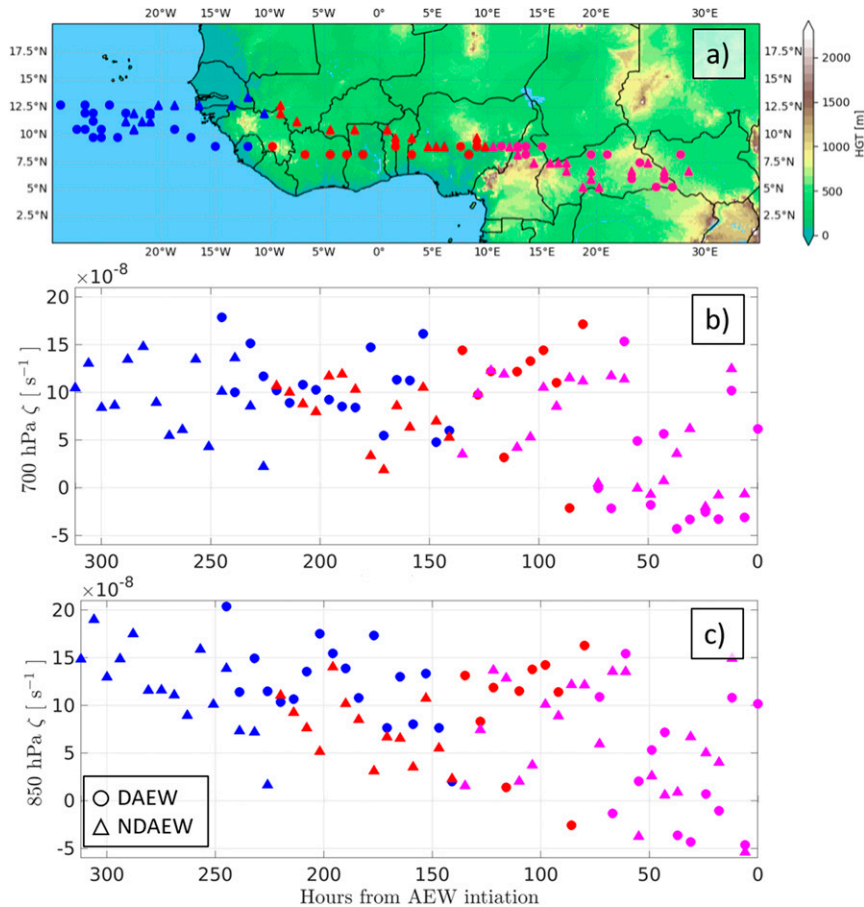
FIG. 11. (a) Tracks of a representative DAEW (circles) and NDAEW (triangles). Also shown are time series for both DAEW and NDAEW of the mean relative vorticity at (b) 700 and (c) 8500 hPa. The position and relative vorticity value over regions A, B, and C are colored in magenta, red, and blue, respectively.

3) larger WAM moisture and convective signature concentrated west of the Marrah Mountains.

Over western Africa, DAEWs experience

1) stronger WAM and
2) more intense and extended AEJ off the west coast of Africa and offshore waters.

These favorable conditions have been related to the potential of the AEWs to undergo TCG downstream of the favorable environment. Significantly, AEWs that initiate over region East and leave the west coast are more probable to undergo TCG than those that initiate over region West and leave the west coast (Table 1). The synoptic features identified here suggest very promising candidate predictors of a possible subsequent TCG event and could inform TCG prediction. These same synoptic conditions can also serve as key rainfall predictors over eastern Africa. We argue that the challenges in TCG prediction, as described by Elless and Torn (2019) and Torn (2010) could be linked to the more intense WAM and AEJ environment for DAEWs that has been isolated in these analyses.

The modulation of the near-trough environment by the larger scales over region East has been shown to be intrinsic to furthering AEW intensification and subsequent TCG. Although having shallower initial circulation, DAEWs have a stronger 850-hPa dynamical and thermodynamic structure (related to the higher WAM moisture availability). They are more likely than NDAEWs to have initiated over region East and to the south of the AEJ; thus, we propose that DAEWs are predominantly southern-track AEWs. The more favorable eastern Africa large-scale conditions for DAEWs are shown to modulate the vertical alignment of the low-level vortex and stronger 850-hPa circulation of the DAEWs in central and West Africa, ultimately leading to TCG off the West African coast. Representative DAEW and NDAEW cases (Fig. 11) reveal that it is moving out of East Africa, in the transition from region A to B, that the intensity of the DAEW begins to surpass that of the NDAEW. Once in region B, DAEWs experience more interactions with deep convective systems than NDAEWs. The deeper wave pouch/vertical alignment of DAEWs over West Africa increases the likelihood that DAEWs will experience MVI: temperature and moisture to be

advected toward the center of the vortex creating a favorable environment for the convection close to the wave to thrive and for a feedback (diabatic PV localization) to strengthen the wave further. These results support the argument of Núñez Ocasio et al. (2020) that MVI is more likely for DAEWs. Therefore, for an AEW to have the optimal chance to undergo TCG it must 1) initiate over East Africa, south of the AEJ, under the effect of a deep WAM that enables an initial intense 850-hPa vortex in an anomalous moist environment, 2) constructively interact with convective systems over central and West Africa, where 3) the convection is favored to be at the center of the trough in order to maintain the vertical alignment of the vortex, which is sustained through MVI, finally resulting in TCG under the influence of a deep and extended AEJ over West Africa.

The results presented in this work confirm the hypothesis of Núñez Ocasio et al. (2020) that DAEWs propagate and grow in a large-scale environment that is more conducive for MCS interactions closer to the wave trough, with a more intense WAM (and possibly located closer to the equatorial belt) and AEJ than is the case for NDAEWs. Optimal mesoscale interactions at the trough center and favorable large-scale conditions at initiation combine to substantially increase likelihood of the formation of a resilient and convectively sustained AEW that subsequently undergoes TCG. We recommend that future work on Atlantic TCG explores further the relationship between DAEWs and an active and wet WAM, and at the same time, how these are related to other seasonal to subseasonal variability such as Madden–Julian oscillation (MJO), El Niño–Southern Oscillation (ENSO), Kelvin waves, and even the North Atlantic Oscillation (NAO).

REFERENCES

Adames, A. F., 2021: Interactions between water vapor, potential vorticity, and vertical wind shear in quasi-geostrophic motions: Implications for rotational tropical motion systems. *J. Atmos. Sci.*, **78**, 903–923, https://doi.org/10.1175/JAS-D-20-0205.1.

——, and Y. Ming, 2018: Interactions between water vapor and potential vorticity in synoptic-scale monsoonal disturbances: Moisture vortex instability. *J. Atmos. Sci.*, **75**, 2083–2106, https://doi.org/10.1175/JAS-D-17-0310.1.

Benjamini, Y., and Y. Hochberg, 1995: Controlling the false discovery rate: A practical and powerful approach to multiple testing. *J. Roy. Stat. Soc.*, **57B**, 289–300, https://doi.org/10.1111/j.2517-6161.1995.tb02031.x.

Berry, G., C. Thorncroft, and T. Hewson, 2007: African easterly waves during 2004—Analysis using objective techniques. *Mon. Wea. Rev.*, **135**, 1251–1267, https://doi.org/10.1175/MWR3343.1.

Brammer, A., and C. D. Thorncroft, 2015: Variability and evolution of African easterly wave structures and their relationship with tropical cyclogenesis over the eastern Atlantic. *Mon. Wea. Rev.*, **143**, 4975–4995, https://doi.org/10.1175/MWR-D-15-0106.1.

——, and ——, 2017: Spatial and temporal variability of the three-dimensional flow around African easterly waves. *Mon. Wea. Rev.*, **145**, 2879–2895, https://doi.org/10.1175/MWR-D-16-0454.1.

——, ——, and J. P. Dunion, 2018: Observations and predictability of a nondeveloping tropical disturbance over the eastern Atlantic. *Mon. Wea. Rev.*, **146**, 3079–3096, https://doi.org/10.1175/MWR-D-18-0065.1.

Cheng, Y.-M., 2019: Variability of African easterly waves. Ph.D. thesis, University at Albany, State University of New York, 173 pp.

——, C. D. Thorncroft, and G. N. Kiladis, 2019: Two contrasting African easterly wave behaviors. *J. Atmos. Sci.*, **76**, 1753–1768, https://doi.org/10.1175/JAS-D-18-0300.1.

Dee, D. P., and Coauthors, 2011: The ERA-Interim reanalysis: Configuration and performance of the data assimilation system. *Quart. J. Roy. Meteor. Soc.*, **137**, 553–597, https://doi.org/10.1002/qj.828.

Dunkerton, T. J., M. T. Montgomery, and Z. Wang, 2009: Tropical cyclogenesis in a tropical wave critical layer: Easterly waves. *Atmos. Chem. Phys.*, **9**, 5587–5646, https://doi.org/10.5194/acp-9-5587-2009.

Duvel, J.-P., 2021: On vortices initiated over West Africa and their impact on North Atlantic tropical cyclones. *Mon. Wea. Rev.*, **149**, 585–601, https://doi.org/10.1175/MWR-D-20-0252.1.

Efron, B., and R. Tibshirani, 1993: *An Introduction to the Bootstrap. Stat. Appl. Probab. Monogr.*, Vol. 57, Chapman and Hall, 436 pp.

Elless, T. J., and R. D. Torn, 2019: Investigating the factors that contribute to African easterly wave intensity forecast uncertainty in the ECMWF ensemble prediction system. *Mon. Wea. Rev.*, **147**, 1679–1698, https://doi.org/10.1175/MWR-D-18-0071.1.

Hamilton, H. L., K. M. Núñez Ocasio, J. L. Evans, G. S. Young, and J. D. Fuentes, 2020: Topographic influence on the African easterly jet and African easterly wave energetics. *J. Geophys. Res. Atmos.*, **125**, e2019JD032138, https://doi.org/10.1029/2019JD032138.

Hankes, I., Z. Wang, G. Zhang, and C. Fritz, 2015: Merger of African easterly waves and formation of Cape Verde storms. *Quart. J. Roy. Meteor. Soc.*, **141**, 1306–1319, https://doi.org/10.1002/qj.2439.

Hopsch, S. B., C. D. Thorncroft, and K. R. Tyle, 2010: Analysis of African easterly wave structures and their role in influencing tropical cyclogenesis. *Mon. Wea. Rev.*, **138**, 1399–1419, https://doi.org/10.1175/2009MWR2760.1.

Janiga, M. A., and C. D. Thorncroft, 2013: Regional differences in the kinematic and thermodynamic structure of African easterly waves. *Quart. J. Roy. Meteor. Soc.*, **139**, 1598–1614, https://doi.org/10.1002/qj.2047.

——, and ——, 2016: The influence of African easterly waves on convection over tropical Africa and the east Atlantic. *Mon.*

Wea. Rev., **144**, 171–192, https://doi.org/10.1175/MWR-D-14-00419.1.

Jones, S. C., 1995: The evolution of vortices in vertical shear. I: Initially barotropic vortices. *Quart. J. Roy. Meteor. Soc.*, **121**, 821–851, https://doi.org/10.1002/qj.49712152406.

Landsea, C. W., A. Hagen, W. Bredemeyer, C. Carrasco, D. A. Glenn, A. Santiago, D. Strahan-Sakoskie, and M. Dickinson, 2014: A reanalysis of the 1931–43 Atlantic Hurricane Database. *J. Climate*, **27**, 6093–6118, https://doi.org/10.1175/JCLI-D-13-00503.1.

Leppert, K. D., D. J. Cecil, and W. A. Petersen, 2013: Relation between tropical easterly waves, convection, and tropical cyclogenesis: A Lagrangian perspective. *Mon. Wea. Rev.*, **141**, 2649–2668, https://doi.org/10.1175/MWR-D-12-00217.1.

Leroux, S., and N. M. J. Hall, 2009: On the relationship between African easterly waves and the African easterly jet. *J. Atmos. Sci.*, **66**, 2303–2316, https://doi.org/10.1175/2009JAS2988.1.

Lin, Y.-L., K. E. Robertson, and C. M. Hill, 2005: Origin and propagation of a disturbance associated with an African easterly wave as a precursor of Hurricane Alberto (2000). *Mon. Wea. Rev.*, **133**, 3276–3298, https://doi.org/10.1175/MWR3035.1.

——, L. Liu, G. Tang, J. Spinks, and W. Jones, 2013: Origin of the pre-Tropical Storm Debby (2006) African easterly wave-mesoscale convective system. *Meteor. Atmos. Phys.*, **120**, 123–144, https://doi.org/10.1007/s00703-013-0248-6.

Matthews, A. J., and G. N. Kiladis, 1999: The tropical–extratropical interaction between high-frequency transients and the Madden–Julian oscillation. *Mon. Wea. Rev.*, **127**, 661–677, https://doi.org/10.1175/1520-0493(1999)127<0661:TTEIBH>2.0.CO;2.

Núñez Ocasio, K. M., J. L. Evans, and G. S. Young, 2020: A wave-relative framework analysis of AEW–MCS interactions leading to tropical cyclogenesis. *Mon. Wea. Rev.*, **148**, 4657–4671, https://doi.org/10.1175/MWR-D-20-0152.1.

Peng, M. S., B. Fu, T. Li, and D. E. Stevens, 2012: Developing versus nondeveloping disturbances for tropical cyclone formation. Part I: North Atlantic. *Mon. Wea. Rev.*, **140**, 1047–1066, https://doi.org/10.1175/2011MWR3617.1.

Pytharoulis, I., and C. Thorncroft, 1999: The low-level structure of African easterly waves in 1995. *Mon. Wea. Rev.*, **127**, 2266–2280, https://doi.org/10.1175/1520-0493(1999)127<2266:TLLSOA>2.0.CO;2.

Raymond, D. J., and C. López Carrillo, 2011: The vorticity budget of developing Typhoon Nuri (2008). *Atmos. Chem. Phys.*, **11**, 147–163, https://doi.org/10.5194/acp-11-147-2011.

Reed, R. J., D. C. Norquist, and E. E. Recker, 1977: The structure and properties of African wave disturbances as observed during phase III of GATE. *Mon. Wea. Rev.*, **105**, 317–333, https://doi.org/10.1175/1520-0493(1977)105<0317:TSAPOA>2.0.CO;2.

Russell, J. O., A. Aiyyer, J. D. White, and W. Hannah, 2017: Revisiting the connection between African easterly waves and Atlantic tropical cyclogenesis. *Geophys. Res. Lett.*, **44**, 587–595, https://doi.org/10.1002/2016GL071236.

Schreck, I., J. Carl, L. Shi, J. P. Kossin, and J. J. Bates, 2013: Identifying the MJO, equatorial waves, and their impacts using 32 years of HIRS upper-tropospheric water vapor. *J. Climate*, **26**, 1418–1431, https://doi.org/10.1175/JCLI-D-12-00034.1.

Schwendike, J., and S. C. Jones, 2010: Convection in an African easterly wave over West Africa and the eastern Atlantic: A model case study of Helene (2006). *Quart. J. Roy. Meteor. Soc.*, **136**, 364–396, https://doi.org/10.1002/qj.566.

Thorncroft, C., and K. Hodges, 2001: African easterly wave variability and its relationship to Atlantic tropical cyclone activity. *J. Climate*, **14**, 1166–1179, https://doi.org/10.1175/1520-0442(2001)014<1166:AEWVAI>2.0.CO;2.

——, N. M. J. Hall, and G. N. Kiladis, 2008: Three-dimensional structure and dynamics of African easterly waves. Part III: Genesis. *J. Atmos. Sci.*, **65**, 3596–3607, https://doi.org/10.1175/2008JAS2575.1.

Torn, R. D., 2010: Ensemble-based sensitivity analysis applied to African easterly waves. *Wea. Forecasting*, **25**, 61–78, https://doi.org/10.1175/2009WAF2222255.1.

Vizy, E. K., and K. H. Cook, 2003: Connections between the summer East African and Indian rainfall regimes. *J. Geophys. Res.*, **108**, 4510, https://doi.org/10.1029/2003JD003452.

Wang, Z., 2018: What is the key feature of convection leading up to tropical cyclone formation? *J. Atmos. Sci.*, **75**, 1609–1629, https://doi.org/10.1175/JAS-D-17-0131.1.

——, M. T. Montgomery, and C. Fritz, 2012: A first look at the structure of the wave pouch during the 2009 PREDICT–GRIP dry runs over the Atlantic. *Mon. Wea. Rev.*, **140**, 1144–1163, https://doi.org/10.1175/MWR-D-10-05063.1.

Zawislak, J., 2020: Global survey of precipitation properties observed during tropical cyclogenesis and their differences compared to nondeveloping disturbances. *Mon. Wea. Rev.*, **148**, 1585–1606, https://doi.org/10.1175/MWR-D-18-0407.1.

——, and E. J. Zipser, 2010: Observations of seven African easterly waves in the east Atlantic during 2006. *J. Atmos. Sci.*, **67**, 26–43, https://doi.org/10.1175/2009JAS3118.1.

——, and ——, 2014: A multisatellite investigation of the convective properties of developing and nondeveloping tropical disturbances. *Mon. Wea. Rev.*, **142**, 4624–4645, https://doi.org/10.1175/MWR-D-14-00028.1.

Zipser, E. J., and Coauthors, 2009: The Saharan air layer and the fate of African easterly waves—NASA's AMMA field study of tropical cyclogenesis. *Bull. Amer. Meteor. Soc.*, **90**, 1137–1156, https://doi.org/10.1175/2009BAMS2728.1.